A transcriptional dissection of the petty spurge (*Euphorbia peplus* L.) reproductive structure

Authors: Arielle Rose Johnson[1*], Ashley Bao[1], Margaret Hannah Frank[1]
Affiliation: [1]Plant Biology Section, School of Integrative Plant Science, Cornell University, Ithaca, NY, USA
*Contact: arj66@stanford.edu

Abstract: The unique reproductive structure of *Euphorbia* species, the cyathium, is an inflorescence that resembles a single complete flower. This structure has not yet been investigated using transcriptomics at a genomic scale. Enabled by the petty spurge (*Euphorbia peplus* L.) genome and guided by the ABCDE model of floral development, we dissected petty spurge cyathia and carried out a transcriptomic analysis of the different organs. We also constructed gene phylogenies and performed dN/dS analysis on select floral genes. Unlike in model species in the Asteraceae, which also have pseudanthia (false flowers), we did not find evidence for lineage-specific duplications of E class genes in *Euphorbia*. Rather, our transcriptomic and genomic analyses indicate that SEP1 paralogs have distinct expression patterns within the cyathium. *E. peplus* filiform structures (sterile organs within the cyathium) show upregulation of B and E class genes and transcriptomic signatures of heterochromatin formation, consistent with some form of floral identity and potentially consistent with their being reduced flowers in an inflorescence. The gene *CRABS CLAW* (*CRC*), which is involved in nectary development in both arabidopsis and petunia, is not upregulated in *E. peplus* nectaries, indicating an alternative nectary development pathway in *Euphorbia.* Finally, *Euphorbia* homologs for the inflorescence/floral meristem genes *UFO* and *LFY* and the B class genes *AP3* and *PI* have highly diverged sequences relative to other Euphorbiaceae species.

Key words: *Euphorbia peplus*, *Euphorbia*, cyathium, spurge, inflorescence

INTRODUCTION

There are approximately 2000 species of *Euphorbia*, including horticulturally important plants such as poinsettia (*Euphorbia pulcherrima* L). The reproductive structure of *Euphorbia* species is called a cyathium. A cyathium resembles a complete flower with pistils, stamens, and a perianth; however, it is a pseudanthium (false flower) that is a condensed inflorescence consisting of a pistillate flower surrounded by staminate flowers and an involucral bract (Figure 1).

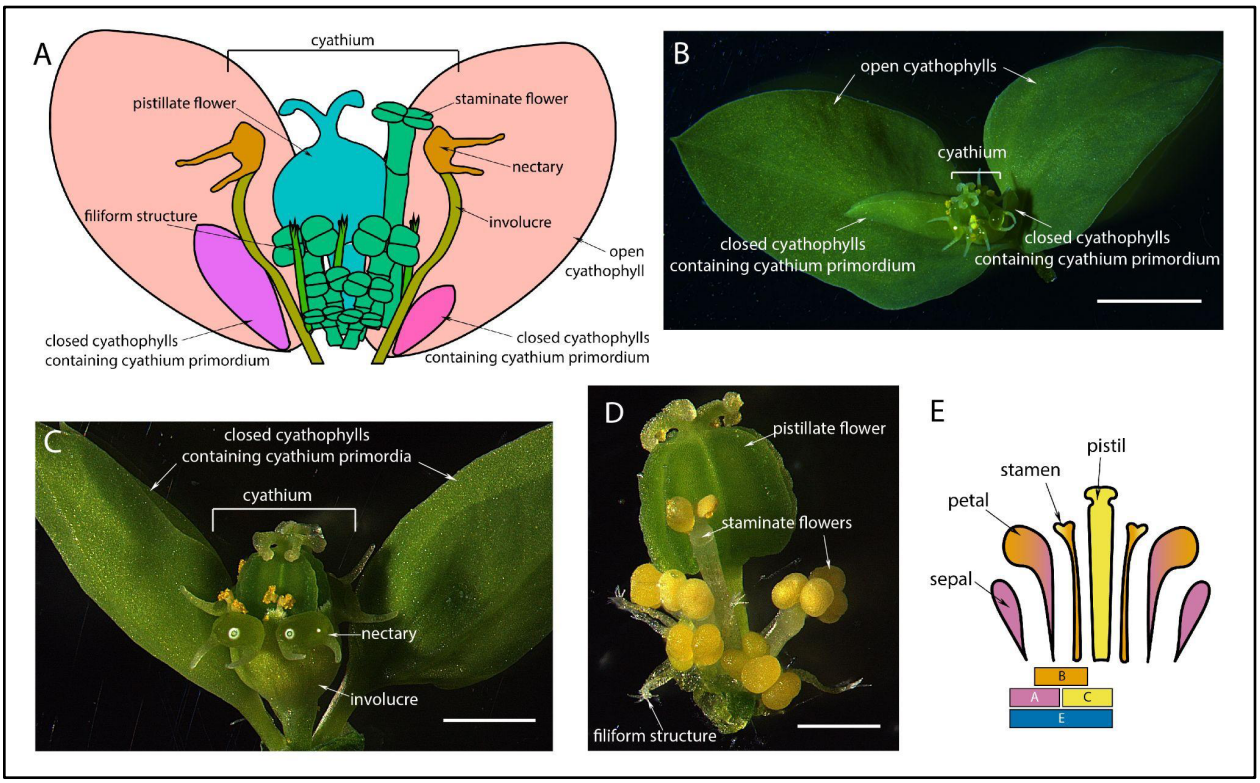

Figure 1

Euphorbia peplus L., commonly known as petty spurge, is an emerging model species for *Euphorbia* with a publicly available genome assembly (Czechowski et al., 2022; Johnson et al., 2023). In *E. peplus*, each immature cyathium is enclosed within two bracts, called cyathophylls. The cyathophyll contains the immature cyathium as well as multiple smaller cyathium primordia

(enclosed in their own cyathophylls). The total number of primordia can vary by ecotype. Although *E. peplus* is primarily self-pollinated, the cyathium remains enclosed by cyathophylls until the stigma is receptive to pollen (indicated by maturation of stigma lobe morphology), which brings the cyathium into the open for pollination and later seed dispersal (Li et al., 2014).

The *E. peplus* cyathium itself, as in other *Euphorbia* species, is composed of a single pistillate flower in the center, surrounded by five mature staminate flowers. Each of the five mature staminate flowers is subtended by immature or nonfunctional staminate flowers in a zigzag pattern. Interspersed with the staminate flowers in the *E. peplus* cyathium are fringed filiform (threadlike) structures. These filiform structures have been referred to by various terms including “filamentous structures” (Prenner and Rudall, 2007) and “filiform bracteoles” (Bruyns, 2022). For the sake of clarity, we will refer to these structures as “filiform structures" in this paper, because “filamentous” implies a developmental homology between these structures and filaments, and because Prenner and Rudall 2007 also refer to cyathophylls as “bracteoles” (Prenner and Rudall, 2007). The pistillate flower, staminate flowers, and filiform structures are surrounded by a fused cuplike structure of involucral bracts, also known as the involucre. It is this cup-shaped structure that gives cyathia their name, as “cyathium” comes from the Greek word for cup, “kyathos”. In *E. peplus*, 4 or 5 crescent-shaped nectaries are present near the top of the involucre.

Although the cyathium has the superficial organization of a single flower (i.e., a pistillate structure surrounded by staminate structures that are surrounded by sterile organs), it is generally interpreted as an inflorescence based on several criteria (reviewed in Prenner and Rudall, 2007). There is a line of constriction on the staminate flower that is interpreted as the flower-stamen boundary, rather than individual stamens. Other genera in the Euphorbiaceae (e.g. *Anthostema*, Figure 2) form distinct staminate flowers that are clustered around a single

pistillate flower. In addition, species within the Euphorbiaceae typically have unisexual flowers, and the bisexual composition of the cyathium would be an exception to this trend (Kaplan and Specht, 2022). Other genera within the Euphorbiaceae, such as *Dalechampia* and *Pera* have reproductive structures that have long been established to be pseudanthia (i.e., inflorescences that resemble single flowers; Gagliardi et al., 2018). Prenner and Rudall 2007 speculate that because the cyathium is an inflorescence, the sterile filiform structures that surround the staminate flowers could be interpreted either as prophylls or as highly reduced staminate flowers from a dichasial inflorescence (Prenner and Rudall, 2007). They interpret the involucre as a non-floral organ.

As compared with its relatives such as *Anthostema* (Figure 2), the *Euphorbia* inflorescence is very compact structurally. Cyathia have a reduced axis, different placement of their flowers, and an earlier emergence of pistillate flower primordia compared with staminate flower primordia than inflorescences of related genera (Gagliardi et al., 2018). The Australian genus *Calycopeplus* and the New Caledonia tree *Neoguillauminia cleopatra* have been proposed as "missing links" towards the evolution of the *Euphorbia* cyathium from separate pistillate and staminate flowers; these close relatives to *Euphorbia* both have an inflorescence where a pistillate flower has its own small perianth that is then surrounded by staminate flowers with their own perianth whorls (Figure 2) (Western Australian Herbarium et al., n.d.; Prenner and Rudall, 2007; Prenner et al., 2008; Dressler et al., 2014; Gilbert, 1994).

Calycopeplus paucifolius © overlander (Gerald Krygsman), iNaturalist | *Neoguillauminia cleopatra* © Benoit Henry, Pl@ntNet | *Anthostema senegalense* © Philippe Birnbaum, African Plants-- A Photo Guide

Figure 2

Now that a high-quality genome is publicly available for two *Euphorbia* species, the cyathium can be investigated from a comparative molecular developmental perspective. This paper will use transcriptomics and evolutionary analysis to shed more light on the cyathium structure. Transcriptomics of floral development of another species in the Euphorbiaceae, *Jatropha curcas* L., showed that the ABCDE model of floral developmental regulation (Irish, 2017) is mostly conserved in *J. curcas* (Hui et al., 2017); therefore, we decided to investigate the ABCDE genes in *Euphorbia* as well.

Under the ABCDE model, different combinations of MADS-box transcription factors combine to specify the four floral whorls: the sepals, petals, stamens, and carpel (Figure 1E). E class genes are present throughout the flower and help specify all four whorls. C class transcription factors specify the carpel; B and C genes together specify stamens; B and A genes together specify the petal; and A genes alone specify the sepal. D class genes specify ovules. Generally, B and C class genes are conserved between taxa, while A class genes are not highly conserved (Litt and Kramer, 2010). Complete flowers contain all of the floral whorls, while

102 unisexual flowers have either functional stamens or functional carpels but not both. As defined
103 by Mitchell and Diggle 2005, unisexual flowers can be classified based on the presence or
104 absence of rudiments of the gynoecium or androecium (Type I = rudiments present; Type II =
105 rudiments absent) (Mitchell and Diggle, 2005). The *Euphorbia* cyathium has Type II unisexual
106 flowers, with no evidence of sterile carpels/stamens present. The complete disappearance of a
107 reproductive whorl in Type II unisexual flowers is hypothesized to result from differential
108 regulation of the MADS-box transcription factors (Feng et al., 2020). The flowers of the
109 *Euphorbia* cyathium also lack a perianth (sepals and petals). Loss of the perianth whorls can
110 result from edits to MADS-box transcription factors or to other transcription factors not related to
111 whorl identity, as is seen in the arabidopsis *petal loss* (*ptl*) mutant (Brewer et al., 2004).
112
113 We also wanted to contextualize the *Euphorbia* cyathium as a pseudanthium (false flower).
114 False flowers can form from multiple types of meristems. Claßen-Bockhoff and Bull-Hereñu
115 2013 use an ontogenetic framework to draw distinctions between two different types of flower-
116 producing meristems: 'flower unit meristems' (FUMs) which are determinate and lack apical
117 growth, and inflorescence meristems (IMs) which are initially indeterminate and show apical
118 growth (Claßen-Bockhoff and Bull-Hereñu, 2013). IMs produce the basic branched
119 inflorescence types, e.g. racemes and panicles, whereas FUMs are relatively similar to floral
120 meristems and generate dense heads of flowers. Head meristems in Asteraceae are considered
121 FUMs based on their mantle-core structure and lack of apical growth (Zhang and Elomaa,
122 2021). Morphological work on *Ricinus communis* (Euphorbiaceae), reinterpreted its "staminate
123 flower" which forms many-branched "staminal trees" as a multi-flower unit with each flower
124 reduced to a single anther, forming from an FUM (Claßen-Bockhoff and Frankenhäuser, 2020).
125 The *Euphorbia* cyathium similarly has a meristem that could be interpreted as an FUM, as it
126 initially lacks visible primordia (Prenner and Rudall, 2007). Because of their ontogenetic
127 similarity, we compared the *Euphorbia* cyathium with the Asteraceae pseudanthium.

128

129 **MATERIALS AND METHODS**

130

131 ***Plant growth conditions***—

132 *E. peplus* plants were grown under long day conditions with 25 °C day/16 °C night. Seeds
133 were germinated without any pretreatment in closed Phytatrays (P5929; Sigma-Aldrich, Saint
134 Louis, MO, USA) in LM 1-1-1 soil mix, then week-old plants were uppotted to 4-inch pots
135 containing LM 1-1-1 soil mix.

136

137 ***Imaging***—

138 Images of cyathia were taken using a Leica M205 FCA stereo microscope with a DMC6200
139 camera.

140

141 ***Fixation and dissection for RNA sequencing***—

142 Cyathia from twelve-week-old *E. peplus* plants were collected into ice-cold acetone then stored
143 at -20°C until dissection. Cyathia were dissected under the dissecting scope in acetone on a
144 cold block and dissected organs were put immediately into chilled acetone tubes. 5 biological
145 replicates of 10 different organs were collected, with 10 cyathia dissected for each biological
146 replicate.

147

148 ***Stages used for RNA sequencing***—

149 We used primordia approximately 200 μm tall for our “small primordium” samples. We used
150 cyathium primordia approximately 500 μm tall for our “large primordium” samples. We used
151 staminate flower primordia approximately 200 μm tall for our “young staminate flowers” and
152 pistillate flower primordia approximately 400 μm tall for our “young pistillate flowers”. For the
153 remaining samples, we dissected them from nearly-mature cyathia still enclosed within

154 unopened cyathophylls when cyathia were approximately 1.5 mm tall not including cyathophylls:
155 nectary, involucre, mature staminate flower, mature pistillate flower, filiform structure. In our
156 organ stages, 'mature' here refers to developmental maturity of form, not reproductive maturity,
157 which roughly coincides with the opening of the cyathophylls. At reproductive maturity, cyathia
158 are approximately 2mm tall.
159
160 ***RNA extraction***—
161 RNA was extracted using the New England Biolabs Monarch Total RNA Miniprep Kit (NEB
162 #T2010, Ipswich, MA, USA). Acetone was removed from the tubes under the dissecting scope,
163 2-3 beads (BioSpec Products #11079124, Bartlesville, OK, USA) were added, the tubes were
164 placed into liquid nitrogen, and the tissue was ground in a bead beater (Qiagen TissueLyser II,
165 Germantown, MD, USA). 400uL of 1x protection reagent from the kit was added to the ground
166 tissue and beads, and the tissue was ground again in the protection reagent. The liquid was
167 transferred to a new tube and the rest of the kit protocol was followed. RNA was eluted with
168 100uL nuclease-free water.
169
170 ***RNA purification***—
171 The 100uL of RNA was purified by adding 10uL 3M sodium acetate, 0.75uL GlycoBlue
172 (ThermoFisher #AM9515, Waltham, MA USA) and 275uL ice-cold 100% ethanol, vortexing to
173 mix, precipitating at -80°C overnight, centrifuging at 13000 rpm at 4°C for 30 minutes, washing
174 the pellet twice with 0.5mL ice-cold 75% ethanol, air-drying the pellet for 5 minutes, and
175 resuspending the RNA in 20uL of nuclease-free water.
176
177 ***3' sequencing***—
178 RNA samples were submitted to the Cornell Institute for Biotechnology Genomics Center for 3'
179 mRNA-seq library construction using a QuantSeq FWD kit (Lexogen, Vienna, Austria) followed

180 by 1x75 bp sequencing on an Illumina NextSeq500 (Illumina, Hayward, CA, USA). Sequencing
181 statistics were calculated with v0.15.0 seqkit stats with parameters -j 10 -T(Shen et al., 2016).
182 (Supplementary File 1).
183
184 ***Orthogroup inference***—
185 To assemble orthogroups, we ran OrthoFinder v2.5.4 (Emms and Kelly, 2019) on the longest
186 isoform protein sequences from *E. peplus*, *E. lathyris*, arabidopsis, soybean, Pará rubber tree,
187 cassava, poplar, and castor bean using the parameters -S diamond -t 40 -a 8(Buchfink et al.,
188 2021). Orthogroups are included in Supplementary File 2.
189
190 ***Identification of ABCDE floral identity genes***—
191 In order to identify floral identity genes of interest, we retrieved the sequences of genes of
192 interest from Uniprot accessed through TAIR and ran blastp with our *E. peplus* proteins file as
193 the query and the parameters -qcov_hsp_perc 80 e-value 1e-10(Camacho et al., 2009). Where
194 BLAST results surfaced multiple candidates with low e-values and high percent identity, a
195 reciprocal BLAST to arabidopsis was used to select the best candidate(s). We further
196 confirmed the results through comparison to the clades identified by OrthoFinder. Gene IDs
197 accessed through TAIR: AT1G69120(AP1)(Bowman et al., 1993); AT4G36920(AP2)(Jofuku et
198 al., 1994); AT3G54340(AP3)(Jack et al., 1992); AT4G18960(AG)(Mizukami and Ma, 1997);
199 AT2G45650(AGL6)(Ma et al., 1991); AT1G69180(CRC)(Alvarez and Smyth, 1999);
200 AT1G65480(FT)(Kobayashi et al., 1999); AT5G60910(AGL8)(Mandel and Yanofsky, 1995);
201 AT5G61850(LFY)(Schultz and Haughn, 1991); AT5G20240(PI)(Goto and Meyerowitz, 1994);
202 AT5G15800(SEP1)(Pelaz et al., 2000); AT1G24260(SEP3)(Pelaz et al., 2000);
203 AT3G58780(SHP1)(Liljegren et al., 2000); AT2G42830(SHP2)(Liljegren et al., 2000);
204 AT2G45660(AGL20)(Lee et al., 2000); AT4G09960(STK)(Favaro et al., 2003);
205 AT5G03840(TFL1)(Kobayashi et al., 1999); AT1G30950(UFO)(Levin and Meyerowitz, 1995).

206

207 ***Transcriptomic analysis***—

208 Raw read files were filtered with fastp v0.23.2 using parameters --cut_right --cut_window_size 5
209 --cut_mean_quality 20 --length_required 50 (Chen et al., 2018). Transcript abundance was
210 generated using *E. peplus* coding sequences with kallisto quant v0.42.4 with parameters --
211 single -b 100 -t 10 (Bray et al., 2016). The resulting data was processed in R using the DESeq2
212 pipeline; all genes with >20 estimated counts across all samples were considered to be
213 expressed and were included in the analysis (Love et al., 2014). Variance-stabilized-
214 transformed data were visualized in heatmaps using the package pheatmap with expression
215 normalized by row and genes clustered by expression pattern (Kolde, n.d.). Of the floral genes
216 of interest investigated (Supplementary File 3), the *E. peplus* homologs for AGL8/FUL
217 (Ep_chr6_g18041), TFL1 (Ep_chr7_g23231) and two paralogs of FT (Ep_chr8_g25489,
218 Ep_chr6_g20489) had expression too low (i.e. 20 or fewer counts across all samples) to be
219 analyzed. Genes are said to be differentially expressed in this paper if padj<0.05. All DESeq
220 filtered untransformed data is included in Supplementary File 4. Comparisons of differentially
221 expressed genes between different tissues are included in Supplementary File 5.

222

223 ***Biological Process and Molecular Function GO term enrichment analysis***—

224 GO terms were assigned to *E. peplus* genes as specified in Johnson et al 2023 (Johnson et al.,
225 2023); GO terms assigned to each gene are included in Supplementary File 6. In order to find
226 which GO terms were enriched in differentially expressed genes in different organs as
227 compared with cyathophylls, we ran TopGO v.2.46.0 using the “classicCount” option, using
228 Fisher’s test to determine significance (Alexa and Rahnenfuhrer, 2021). TopGO results are
229 included in Supplementary File 7. We summarized and visualized the GO results using
230 REVIGO and downloaded the R scripts to edit the color scale and axis limits (Supek et al.,
231 2011). Terms with a dispensability higher than 0.9 were removed and clustered with other

232 terms for ease of visualization. Only terms with a dispensability less than 0.2 were labeled with
233 text in the visualization.
234
235 ***Manual curation of OrthoFinder clades***—
236 Genes with highly truncated annotations were removed from the analysis (LFY: rubber tree
237 KAF2311631.1, soybean Glyma.04G202002.1.p; PHYA: soybean Glyma.03G227333.1.p; PI: *E.*
238 *lathyris* Casp05761.t1; SEP1: rubber tree KAF2325472.1). For PI, *E. lathyris* Casp33119.t1 and
239 *E. peplus* Ep_chr8_g25689.t1 were included in the PI phylogenetic analysis despite being
240 classified into their own orthogroup because they clearly were a result of a tandem duplication
241 (Casp33120.1 and Ep_chr8_g25690.t1 were included in the orthogroup with Arabidopsis PI,
242 AT5G20240.1) and because of high reciprocal BLAST scores with Arabidopsis PI.
243
244 ***Gene alignment, gene tree construction and selection analysis***—
245 For each clade of interest (generated by OrthoFinder then manually curated as specified above;
246 see Supplementary File 3 for gene names), a preliminary alignment was generated using
247 MAFFT v7.522 with parameters --maxiterate 5000 --auto --adjustdirectionaccurately --thread 8 --
248 op 3. Then macse v2.07 alignSequences was used to generate a codon-aware alignment with
249 default parameters. For a few alignments, macse generated exclamation points due to
250 sequencer errors; these were converted to N. Then alignment trimming was performed in trimAl
251 v1.4 with parameter -gappyout. Finally, sequences were exported for phylogeny construction
252 using macse v2.07 exportAlignment -codonForFinalStop NNN -codonForInternalStop NNN -
253 keep_gap_only_sites_ON. To generate phylogenetic trees, RAxML NG v1.2.0 was run with
254 parameters --all --model GTR+G --threads 12 --bs-trees 1000(Kozlov et al., 2019). In order to
255 generate dN/dS values for each branch of the tree, PAML v4.10.6 was run on the best tree from
256 RAxML with model=1 and NSSites=0. In order to test for relaxed selection at sites within
257 genes, PAML v4.10.6 was run on the best tree from RAxML with model=2 and NSSites=2.

258 Alignments were visualized in ESPript 3.0 online (https://espript.ibcp.fr/ESPript/cgi-
259 bin/ESPript.cgi)(Robert and Gouet, 2014). Sites flagged for positive selection based on the
260 Bayes empirical Bayes method (BEB) are included in Supplementary File 8.
261
262 ***Motif analysis***—
263 In order to retrieve a dataset that could be used to detect the canonical LFY binding motif, a bed
264 file of LFY ChIPseq targets (ChIPseq MACS2 q-value 10-10, DANPOS Mnase-seq q-value 10-
265 50) was taken from Supplementary Data 1 from Jin et al 2021 (Jin et al., 2021). This was
266 converted to a fasta file of the target sequences using bedtools getfasta (Quinlan and Hall,
267 2010). Then MEME-ChIP from MEME v5.5.2 was used to detect the LFY canonical binding
268 motif using default parameters except -maxw 25 (Machanick and Bailey, 2011). The dLUBS
269 and mLUBS motifs were acquired from the authors of Rieu et al 2023 in pfm format and
270 converted to meme format using jaspar2meme -pfm from MEME v4.11.2 (Bailey et al., 2015;
271 Rieu et al., 2023b). Then FIMO from MEME v5.5.2 was run with default parameters on a fasta
272 file of the 3kb upstream of the start of the LFY target genes AP1, AG, AP3, and PI in order to
273 assess whether the motifs were present or not (Grant et al., 2011). MEME FIMO motif search
274 results are included in Supplementary File 9.
275
276 ***Genome assemblies used for analysis***—
277 The Johnson et al *Euphorbia peplus* genome assembly and annotation was accessed through
278 Zenodo (Johnson et al., 2023): https://zenodo.org/records/8033914 The Wang et al. *Euphorbia*
279 *lathyris* assembly and annotation was accessed through figshare (Wang et al., 2021):
280 https://figshare.com/articles/dataset/High-
281 quality_genome_assembly_of_the_biodiesel_plant_Euphorbia_lathyris/14909913/1 The Liu et
282 al. *Hevea brasiliensis* (rubber tree) assembly and annotation was accessed through NCBI (Liu
283 et al., 2020): https://www.ncbi.nlm.nih.gov/assembly/GCA_010458925.1/. The Xu et al. wild

284 *Ricinus communis* assembly and annotation was accessed through NCBI (Xu et al., 2021):
285 https://www.ncbi.nlm.nih.gov/datasets/genome/GCF_019578655.1/. The Bredeson et al.
286 *Manihot esculenta* v8.1 assembly and annotation was accessed through Phytozome:
287 https://phytozome-next.jgi.doe.gov/info/Mesculenta_v8_1 The arabidopsis Araport 11 genome
288 release was accessed through TAIR (Cheng et al., 2017):
289 https://www.arabidopsis.org/download/index-
290 auto.jsp?dir=%2Fdownload_files%2FGenes%2FAraport11_genome_release%2FAraport11_bla
291 stsets. The *Glycine max* (soybean) Wm82.a4.v1 assembly and annotation was accessed
292 through Phytozome (Valliyodan et al., 2019): https://phytozome-
293 next.jgi.doe.gov/info/Gmax_Wm82_a4_v1. The *Populus trichocarpa* v4.1 assembly and
294 annotation was accessed through Phytozome (Tuskan et al., 2006): https://phytozome-
295 next.jgi.doe.gov/info/Ptrichocarpa_v4_1
296
297
298 **RESULTS**
299
300 ***Analysis of ABCDE gene expression in cyathium components***—
301 We dissected the different organs of the cyathium and sequenced their RNA (Figure 3 A-D). Of
302 25,473 annotated *E. peplus* genes, 17,164 were expressed in the cyathium. Staminate flowers
303 had the most distinct expression pattern from other organs; a clear separation is visible between
304 the mature staminate flowers, young staminate flowers, and other cyathium organs in the first
305 principal component (PC) of the data (Figure 3E). This data is consistent with many other
306 flowering plant species' transcriptomic pattern of distinct staminate flowers compared with other
307 organs, or distinct stamens compared with other floral organs in complete flowers (Klepikova et
308 al., 2015; Xanthopoulou et al., 2021).

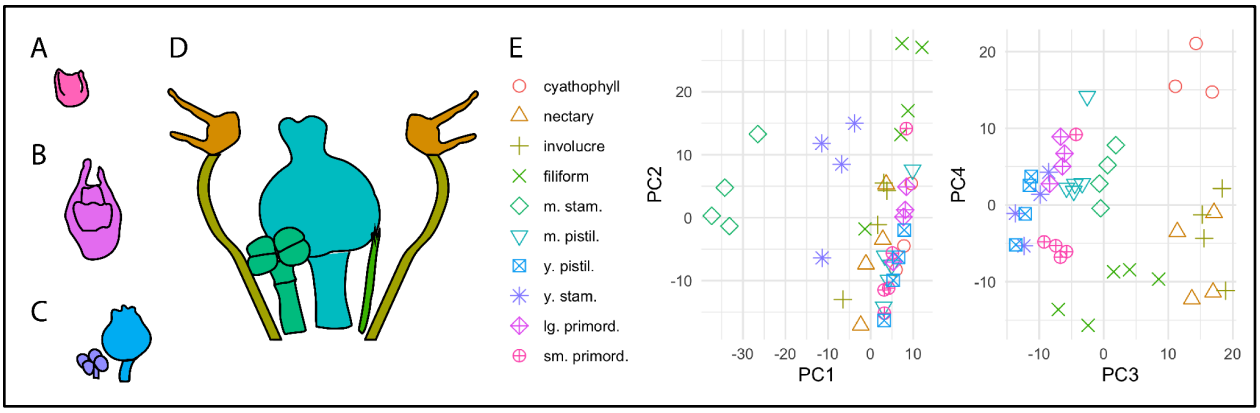

Figure 3

Using BLAST and OrthoFinder, we identified *E. peplus* homologs for all classes of the ABCDE genes and visualized their expression pattern across different organs (Figure 4).

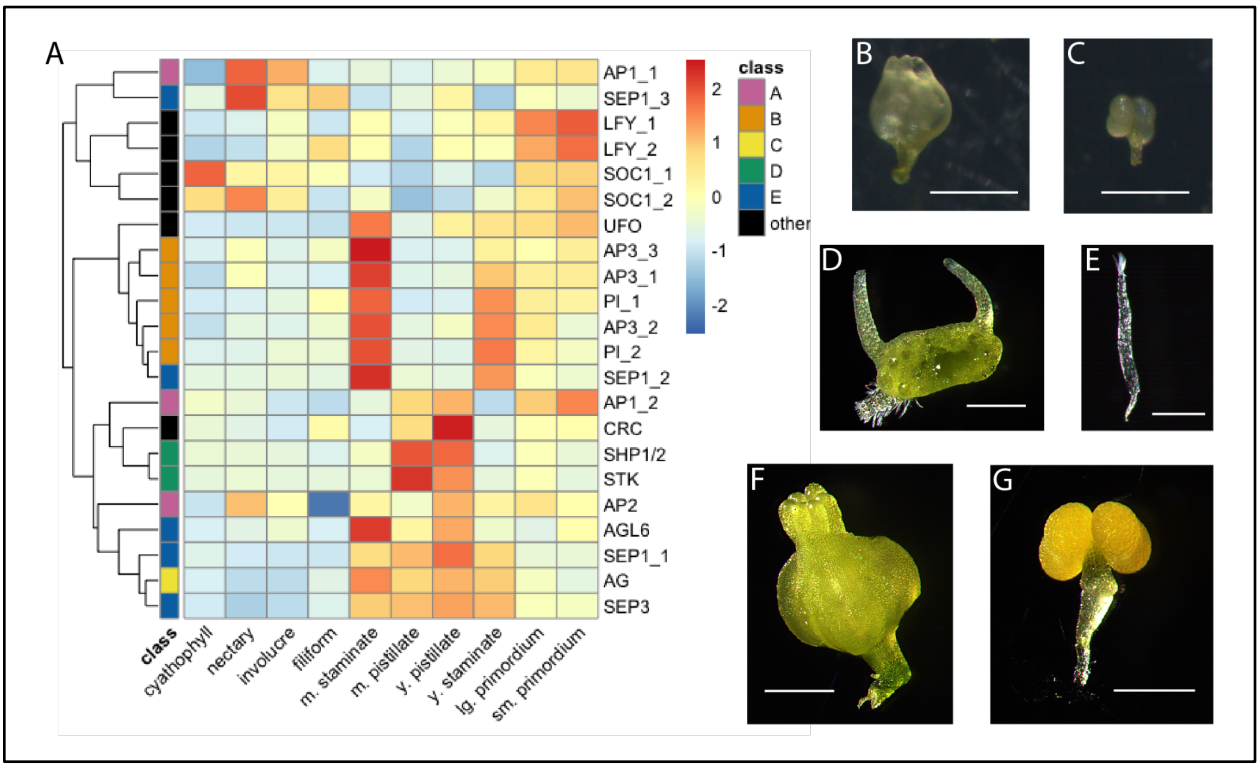

Figure 4

318 In the ABCDE model, the E class genes SEPALLATA1 (SEP1) and SEPALLATA3 (SEP3) are
319 partially redundant in function and help specify all four floral whorls; a closely related E class
320 gene, AGAMOUS-LIKE 6 (AGL6), also helps specify all of the floral organs and is also involved
321 floral meristem regulation (Dreni and Zhang, 2016; Morel et al., 2019). There are three
322 orthologs of SEP1 in *Euphorbia*, which is consistent with other Euphorbiaceae (Supplementary
323 Figure 1). *E. peplus* SEP1_1 is significantly upregulated in both stages of pistillate flowers
324 compared with cyathophylls, SEP1_2 is significantly upregulated in staminate flowers as
325 compared with pistillate flowers, and SEP 1_3 is significantly upregulated in the filiform
326 structures as compared with cyathophylls (Figure 4, Supplementary File 5). *Euphorbia*'s sole
327 SEP3 ortholog is significantly upregulated in both stages of the pistillate and staminate flowers,
328 both stages of the primordia, and the filiform structures as compared with cyathophylls. AGL6 is
329 not significantly expressed in any tissue as compared with the cyathophylls due to low
330 expression overall (Supplementary File 4, Supplementary File 5).
331
332 The B class genes APETALA3 (AP3) and PISTILLATA (PI) specify petal and stamen identity;
333 this role is conserved across bisexual and unisexual flowers (Litt and Kramer, 2010; Zhang et
334 al., 2022). All three *E. peplus* AP3 paralogs and both PI paralogs are significantly upregulated
335 in staminate flowers compared with pistillate flowers at both stages studied, in mature staminate
336 flowers as compared with cyathophylls, in young staminate flowers as compared with
337 cyathophylls (except AP3_3), and in filiform structures as compared with cyathophylls (Figure 4,
338 Supplementary File 5). Of the AP3 and PI homologs, only AP3_2 is significantly expressed in
339 the involucres as compared with the cyathophylls.
340
341 The C class gene AGAMOUS (AG) is deeply conserved across evolution and helps specify both
342 pistillate and staminate development (Dreni and Kater, 2014). The *E. peplus* ortholog of AG is
343 significantly upregulated in both stages of both pistillate flowers and staminate flowers as

344 compared with cyathophylls, and not significantly upregulated in any other parts of the cyathium
345 (Figure 4, Supplementary File 5).
346
347 In arabidopsis, the A class genes APETALA1 (AP1) and APETALA2 (AP2) help specify sepals
348 and help specify petals in conjunction with B class genes, in addition to other functions in floral
349 meristem identity and determinacy (Han et al, 2014). Notably, these genes' functions are not
350 conserved outside the Brassicaceae and are unlikely to be the same in *Euphorbia* as in
351 arabidopsis (Litt and Kramer, 2010; Zumajo-Cardona and Pabón-Mora, 2016). There are two
352 homologs of arabidopsis AP1 in *E. peplus*. AP1_1, which is most similar in sequence to
353 arabidopsis AP1 and CAULIFLOWER (Supplementary Figure 2), is upregulated in the nectary,
354 involucre, filiform structures, both stages of primordia, both stages of staminate flowers, and
355 young pistillate flowers as compared with cyathophylls (Figure 4, Supplementary File 5). *E.*
356 *peplus* AP1_2 and AP2 are not significantly differentially expressed in any cyathium part as
357 compared with cyathophylls, likely due to low gene expression (Supplementary File 4,
358 Supplementary File 5).
359
360 We were also interested in the genes LEAFY (LFY) and UNUSUAL FLORAL ORGANS (UFO)
361 which are known to directly activate many of the ABCDE genes. LFY is a transcription factor
362 that is a key regulator of floral meristem and floral organ identity (Moyroud et al., 2010); it opens
363 up the chromatin around the ABCDE genes, enabling their transcription (Jin et al., 2021). In
364 arabidopsis, UFO interacts with LFY to activate the B class genes AP3 and PI as well as other
365 targets (Rieu et al., 2023b). In some species such as petunia, UFO is also required in addition
366 to LFY to promote floral meristem identity (Souer et al., 2008). *E. peplus* has two homologs of
367 LFY: LFY1_1 is significantly upregulated in both stages of primordia as compared with
368 cyathophylls, and LFY_2 is significantly upregulated in small primordia and filiform structures as
369 compared with cyathophylls (Figure 4, Supplementary File 5). *E. peplus* UFO is upregulated in

370 both stages of primordia, both stages of staminate flowers, young pistillate flowers, and in
371 filiform structures, as compared with cyathophylls. It is significantly upregulated in mature
372 staminate flowers as compared with mature pistillate flowers.
373
374 The gene CRABS CLAW (CRC), which is necessary for nectary development in both
375 arabidopsis and petunia (Morel et al., 2018; Slavković et al., 2021), is not upregulated in *E.*
376 *peplus* nectaries as compared with cyathophylls (Figure 4, Supplementary File 5), suggesting
377 an alternative nectary development pathway in *E. peplus*. It is significantly upregulated in both
378 stages of pistillate flowers as well as in filiform structures compared with cyathophylls, and
379 significantly upregulated in both stages of pistillate flowers compared with staminate flowers.
380 The upregulation of CRC in pistillate flowers in *E. peplus* is consistent with CRC's other
381 functions in carpel development and meristem termination and with results from *J. curcas*,
382 where CRC is highly upregulated during developmental stages of pistillate flowers (Xu et al.,
383 2016).
384
385 ***Transcriptomic analysis of differentially expressed genes in cyathium components***
386
387 We also wanted to investigate what made different parts of the cyathium unique beyond the
388 curated list of floral genes we had selected. Therefore, we performed a gene ontology (GO)
389 term analysis on the genes significantly upregulated in mature staminate flowers, mature
390 pistillate flowers, young staminate flowers, young pistillate flowers, involucres, filiform structures,
391 and nectaries as compared with cyathophylls (Supplementary File 7). We visualized the result
392 for nectaries, involucres, and filiform structures based on semantic similarity of the GO terms
393 (Figure 5).
394

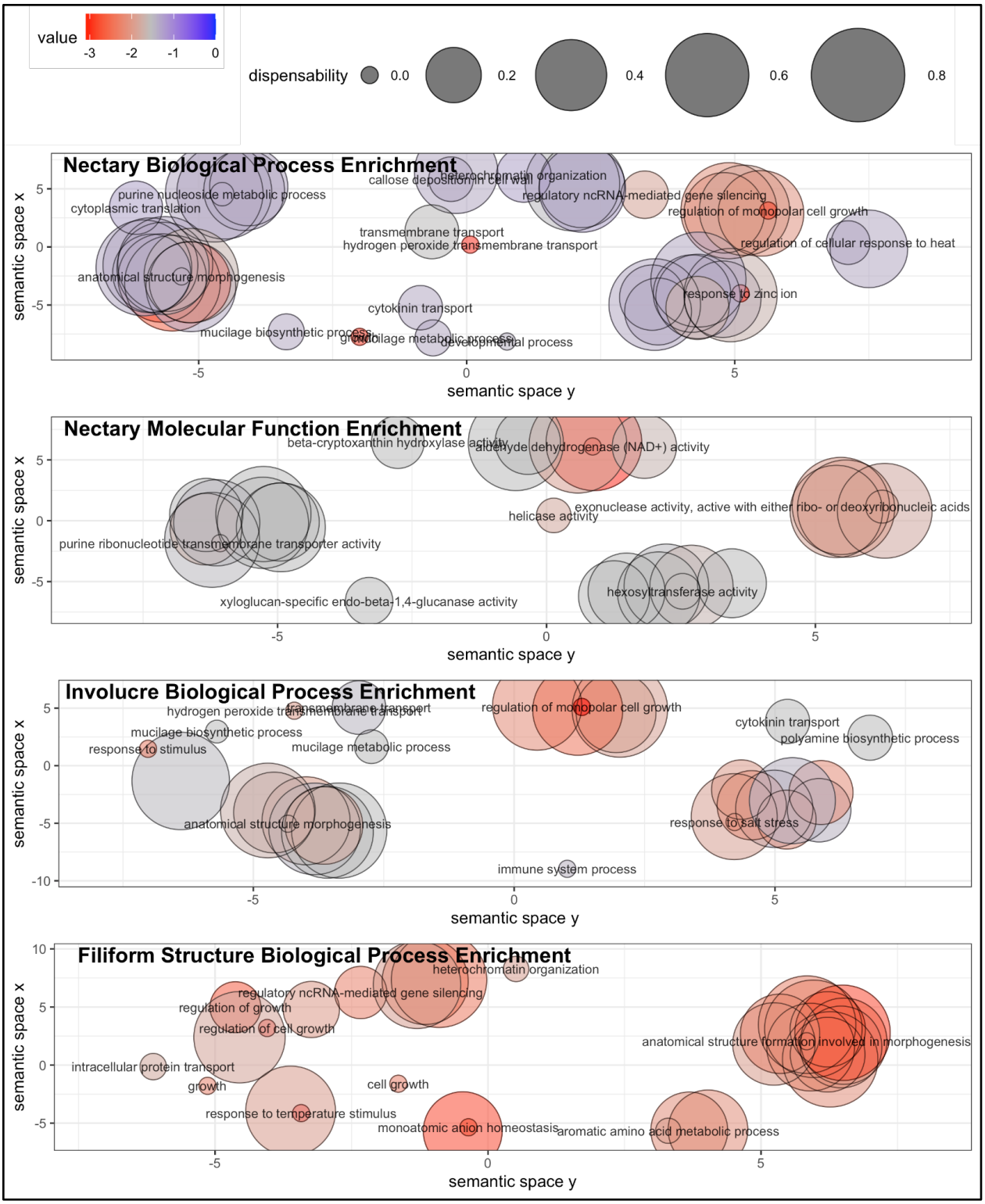
value
-3
-2
-1
0
dispensability
0.0
0.2
0.4
0.6
0.8
Nectary Biological Process Enrichment
purine nucleoside metabolic process
cytoplasmic translation
callose deposition in cell wall
heterochromatin organization
regulatory ncRNA-mediated gene silencing
regulation of monopolar cell growth
transmembrane transport
hydrogen peroxide transmembrane transport
regulation of cellular response to heat
anatomical structure morphogenesis
response to zinc ion
cytokinin transport
mucilage biosynthetic process
mucilage metabolic process
developmental process
semantic space x
semantic space y
Nectary Molecular Function Enrichment
beta-cryptoxanthin hydroxylase activity
aldehyde dehydrogenase (NAD+) activity
exonuclease activity, active with either ribo- or deoxyribonucleic acids
helicase activity
purine ribonucleotide transmembrane transporter activity
hexosyltransferase activity
xyloglucan-specific endo-beta-1,4-glucanase activity
semantic space x
semantic space y
Involucre Biological Process Enrichment
hydrogen peroxide transmembrane transport
regulation of monopolar cell growth
cytokinin transport
polyamine biosynthetic process
mucilage biosynthetic process
response to stimulus
mucilage metabolic process
anatomical structure morphogenesis
response to salt stress
immune system process
semantic space x
semantic space y
Filiform Structure Biological Process Enrichment
heterochromatin organization
regulatory ncRNA-mediated gene silencing
regulation of growth
regulation of cell growth
anatomical structure formation involved in morphogenesis
intracellular protein transport
growth
cell growth
response to temperature stimulus
monoatomic anion homeostasis
aromatic amino acid metabolic process
semantic space x
semantic space y

Figure 5

398 We found that genes upregulated in the nectary as compared with cyathophylls were
399 significantly enriched for multiple Biological Process GO terms relating to transmembrane
400 transport and specialized metabolism (Figure 5, Supplementary File 7). GO terms relating to
401 gene silencing were also enriched. The Molecular Function GO terms enriched in the nectary
402 included multiple significant terms relating to transmembrane transporter activity and
403 glycosyltransferase activity, similarly to the Biological Process GO terms. ATP and NADH
404 metabolism-related terms were also significantly enriched in the nectaries, suggesting an
405 enrichment in energy-generating redox activities.
406
407 Genes upregulated in involucres as compared with cyathophylls were also significantly enriched
408 in genes with Biological Process GO terms relating to specialized metabolite biosynthesis and
409 transmembrane transport (Figure 5, Supplementary File 7). This could potentially indicate that
410 some of the compounds present in the nectaries are at least partially biosynthesized in the
411 involucre tissue connected to the nectaries. The involucre also had several significant GO
412 terms relating to stress, immune responses, and defense responses. The defense GO category
413 may be enriched because of shared hormonal signaling between defense and development; for
414 example, the gene Ep_chr4_g10976, which is upregulated in involucres, is in an orthogroup with
415 AT1G31770(ABCG14), a transmembrane cytokinin transporter. Cytokinin is involved in
416 responses to osmotic stress, salt stress, and other environmental factors but also regulates
417 developmental processes such as inflorescence branching in *J. curcas* (Chen et al., 2019).
418
419 The involucre-upregulated gene with the highest p-value, Ep_chr5_g16200, is in an orthogroup
420 with AT5G03680, PETAL LOSS (PTL), which generally represses tissue growth by limiting cell
421 division (Supplementary File 2). (Despite its name, PTL does not regulate petal organ identity,
422 and its expression is not limited to petals– *ptl* mutants' lack of petals may be due to indirect
423 effects of tissue overgrowth disrupting auxin maxima (O'Brien et al., 2015; Takeda et al., 2022).)

424 This gene is upregulated in filiform structures, young pistillate flowers, mature pistillate flowers,
425 nectaries, and both stages of primordia as compared with cyathophylls (Supplementary File 5),
426 suggesting functions in patterning across multiple cyathium components.
427
428 For the genes upregulated in filiform structures as compared with cyathophylls, stamen
429 development Biological Process GO terms were significantly enriched (Figure 5, Supplementary
430 File 7). Heterochromatin formation, gene silencing, and DNA methylation-related terms were
431 also all significantly enriched.
432
433 The mature staminate flowers had multiple significant Biological Process GO terms for stamen
434 identity and morphogenesis as well as ATP and NADPH related terms (Supplementary File 7).
435 The young staminate flowers had multiple significant GO terms associated with stamen and
436 pollen development but did not have significant ATP or NADPH related terms. The mature
437 pistillate flowers had two GO terms associated with petal development; the pistillate flower-
438 enriched gene causing this significant GO hit, Ep_chr1_g00250, is in an orthogroup with
439 arabidopsis AT4G16850, KronbladStorleK (KSK; the name is Swedish for petal size) which
440 influences auxin responses during petal development (Miller et al., 2020). Compared with the
441 mature pistillate flower, the younger pistillate flower was enriched for more GO terms relating to
442 reproductive structure development, suggesting that the patterning of the pistillate flower is
443 more active in this earlier stage. Both stages of both the pistillate and staminate flowers had
444 significant GO terms relating to gene silencing; the top five most significant mature pistillate
445 flower terms were all related to gene silencing.
446
447 The zinc finger motif-containing gene Ep_chr4_g09148 was in the top 10 most significant
448 upregulated genes in the involucre, nectary, and filiform structures, and was significantly
449 upregulated in every other cyathium tissue studied compared with the involucre (Supplementary

450 File 5). This gene shares an orthogroup with AT2G33835, FRIGIDA-ESSENTIAL 1 (FES1)
451 which is part of a complex that represses flowering in arabidopsis (Schmitz et al., 2005).
452
453 ***Evolutionary analysis of ABCDE floral identity gene sequences***—
454 Changes in MADS-box binding partners are a driver of floral morphological diversity across
455 many plant families (Bartlett, 2017). For example, duplication and neofunctionalization of SEP
456 genes is involved in the generation of pseudanthia in the Asteraceae (Zhang et al., 2017).
457 Therefore, in addition to analyzing gene expression, we analyzed gene sequence evolution in
458 order to see whether there were changes in *Euphorbia* gene sequence and/or copy number that
459 might reflect changes in binding and function. We performed a codon-aware alignment, tree
460 construction, and dN/dS analysis using the gene sequences from *E. peplus*, *Euphorbia lathyris*,
461 several other Euphorbiaceae species, and the model systems arabidopsis, soybean, and poplar
462 (Figure 6, Supplementary Figure 1, Supplementary Figure 2, Supplementary Figure 3).

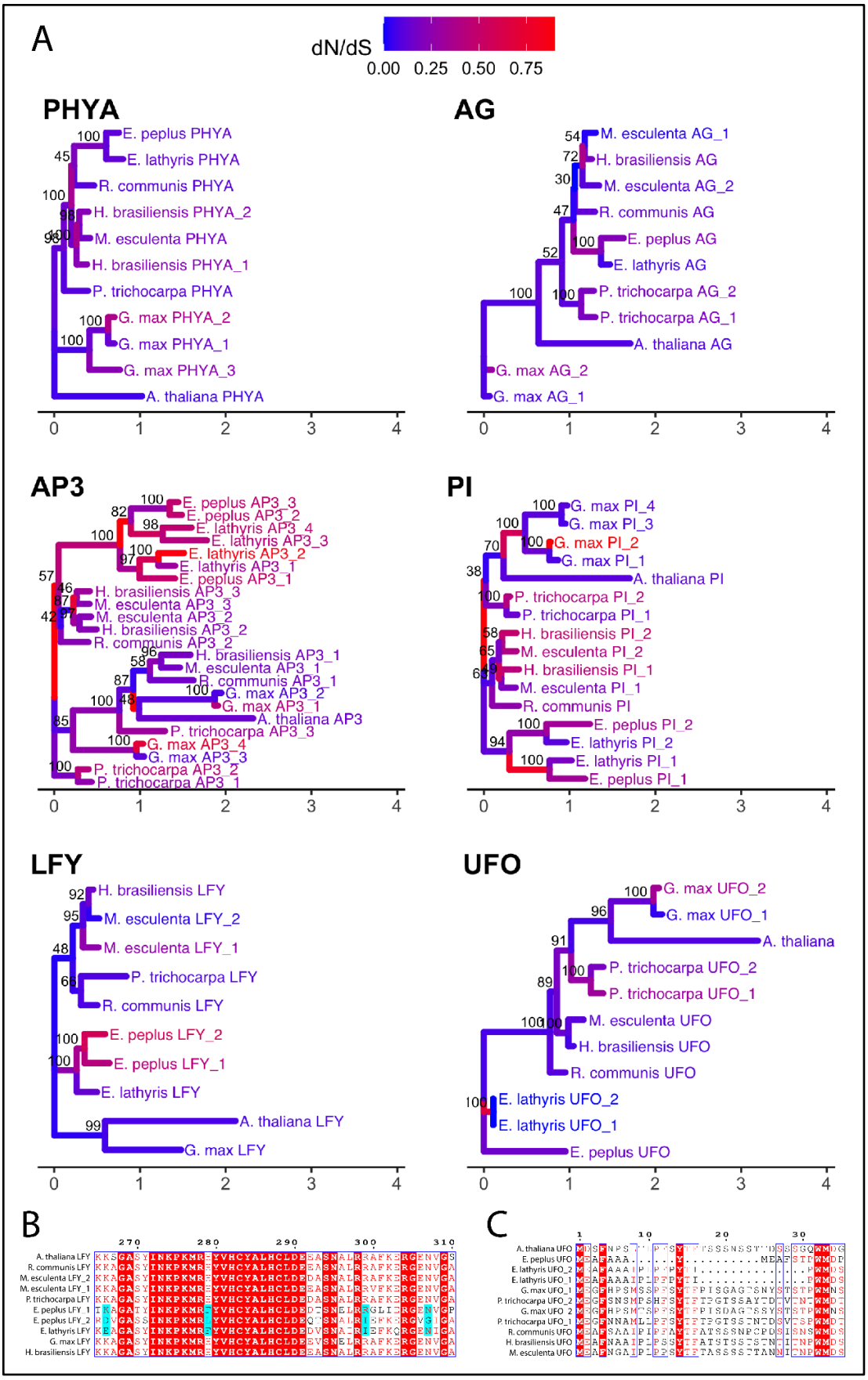
A
dN/dS
0.00 0.25 0.50 0.75
PHYA
E. peplus PHYA
E. lathyris PHYA
R. communis PHYA
H. brasiliensis PHYA_2
M. esculenta PHYA
H. brasiliensis PHYA_1
P. trichocarpa PHYA
G. max PHYA_2
G. max PHYA_1
G. max PHYA_3
A. thaliana PHYA
AG
M. esculenta AG_1
H. brasiliensis AG
M. esculenta AG_2
R. communis AG
E. peplus AG
E. lathyris AG
P. trichocarpa AG_2
P. trichocarpa AG_1
A. thaliana AG
G. max AG_2
G. max AG_1
AP3
E. peplus AP3_3
E. peplus AP3_2
E. lathyris AP3_4
E. lathyris AP3_3
E. lathyris AP3_2
E. lathyris AP3_1
E. peplus AP3_1
H. brasiliensis AP3_3
M. esculenta AP3_3
M. esculenta AP3_2
H. brasiliensis AP3_2
R. communis AP3_2
H. brasiliensis AP3_1
M. esculenta AP3_1
R. communis AP3_1
G. max AP3_2
G. max AP3_1
A. thaliana AP3
P. trichocarpa AP3_3
G. max AP3_4
G. max AP3_3
P. trichocarpa AP3_2
P. trichocarpa AP3_1
PI
G. max PI_4
G. max PI_3
G. max PI_2
G. max PI_1
A. thaliana PI
P. trichocarpa PI_2
P. trichocarpa PI_1
H. brasiliensis PI_2
M. esculenta PI_2
H. brasiliensis PI_1
M. esculenta PI_1
R. communis PI
E. peplus PI_2
E. lathyris PI_2
E. lathyris PI_1
E. peplus PI_1
LFY
H. brasiliensis LFY
M. esculenta LFY_2
M. esculenta LFY_1
P. trichocarpa LFY
R. communis LFY
E. peplus LFY_2
E. peplus LFY_1
E. lathyris LFY
A. thaliana LFY
G. max LFY
UFO
G. max UFO_2
G. max UFO_1
A. thaliana
P. trichocarpa UFO_2
P. trichocarpa UFO_1
M. esculenta UFO
H. brasiliensis UFO
R. communis UFO
E. lathyris UFO_2
E. lathyris UFO_1
E. peplus UFO
B
C

463

464 Figure 6

465

466 LFY, UFO, AP3, and PI show high sequence divergence in *Euphorbia* (Figure 6A). Compared
467 with the non-floral gene PHYTOCHROME A (PHYA) and with the C class gene AG, the genes
468 LFY, AP3, and PI have high dN/dS on their *Euphorbia* branches. The *E. peplus* and *E. lathyris*
469 homologs for LFY have an amino acid change from a positive amino acid to a hydrophobic
470 amino acid in a DNA-binding site that is otherwise deeply conserved in vascular plant lineages
471 dating back to the lycophytes (Figure 6B) (Rodríguez-Pelayo et al., 2022). The *E. peplus* and *E.*
472 *lathyris* homologs for UFO also differ greatly in sequence from other Euphorbiaceae homologs
473 of UFO, and one reason is that the *Euphorbia* versions have deletions near the start of the
474 protein (Figure 6C). Interestingly, many of the AP3 residues flagged as "highly significant" for
475 positive selection in *Euphorbia* are in the K domain in a region involved in tetramer formation
476 (Lai et al., 2019), perhaps indicating a change in binding partner (Supplementary Figure 3).

477

478 Because LFY and UFO showed a high level of sequence divergence, in order to investigate
479 whether LFY and UFO binding targets were conserved, we looked for LFY binding motifs and
480 LFY-UFO binding motifs in the putative promoters of homologs of the LFY targets AP3, PI, AG,
481 and AP1 in *E. peplus*, *H. brasiliensis*, and arabidopsis. (AP3 and PI are targets of the LFY-UFO
482 complex as well.) We hypothesized that the binding motifs might not be conserved in *E. peplus*.
483 Both canonical LFY binding motifs and UFO-LFY motifs (mLUBS and dLUBS) are present in the
484 3kb upstream of these target genes in *E. peplus* (Supplementary File 9), suggesting that at least
485 some of the binding motifs of LFY and LFY-UFO are conserved despite the high divergence in
486 sequence.

487

488 **DISCUSSION**

489

490 Few pseudanthia have been well-characterized at the molecular level. Several studies have
491 examined transcriptional patterns and key developmental genes in the pseudanthium of gerbera
492 (*Gerbera hybrida*, Asteraceae), which has a flower unit meristem (FUM) that lacks apical
493 growth, initially lacks visible primordia, and fractionates into many flowers in a short
494 developmental span—similarly to *Euphorbia*'s cyathium FUM. In the ABCDE model, E-function
495 SEP genes generally promote floral identity. Gerbera has eight SEP homologs due to lineage-
496 specific gene duplications in both the SEP1 and SEP3 subclades; and genes in both subclades
497 have functionally diversified in terms of which floral organs they help specify in the gerbera
498 pseudanthium (Zhang et al, 2017). Interestingly, *Euphorbia* only has four SEP homologs and
499 they are not the result of *Euphorbia*-specific duplications (Supplementary Figure 1), indicating
500 that SEP gene family duplication may not have contributed as much to the development of a
501 pseudanthium in *Euphorbia* as in the Asteraceae. However, the *Euphorbia* SEP homologs do
502 show distinct expression patterns within the cyathium, with the three *Euphorbia* SEP1 homologs
503 all showing different expression patterns from each other. This is consistent with a broader
504 trend that SEP1 orthologs have been repurposed in many species to regulate bract identity and
505 inflorescence architecture (Dreni and Ferrándiz, 2022).
506
507 LFY and UFO are generally important in specifying floral meristem identity (Rieu et al., 2023a;
508 Weigel et al., 1992; Levin and Meyerowitz, 1995, Lippman et al., 2008), although this is not
509 necessarily true for pseudanthia. in gerbera, GhLFY is uniformly expressed in the
510 undifferentiated FUM and regulates its determinacy, while GhUFO is expressed in emerging
511 flower primordia and regulates floral meristem identity (Zhao et al, 2016). The LFY homolog in
512 *J. curcas* (Euphorbiaceae) does promote floral meristem identity; its overexpression causes
513 early flowering, and its co-suppression delays flower formation, promotes more inflorescence
514 branching, and the formation of sepal-like organs (Tang et al., 2016). Although our dataset
515 lacks the spatial and temporal resolution needed at the earliest time points to distinguish which

516 genes are expressed in the cyathium FUM as opposed to the floral meristems, both LFY and
517 UFO are expressed highly in our small primordium and large primordium stage suggesting that
518 they are both important in floral meristem and/or cyathium FUM identity.
519
520 In our analysis of gene sequence evolution, *Euphorbia* LFY, UFO, and the B-class genes AP3
521 and PI show signs of divergence based on phylogenetic distance and relaxed selection. Except
522 for UFO (which may have lacked signs of relaxed selection due to the gene tree topology),
523 these genes also had multiple sites that were classified as highly significant for positive
524 selection in Bayes Empirical Bayes (BEB) analysis (Supplementary File 8). The increased rates
525 of molecular evolution of AP3 and PI in *Euphorbia* is consistent with increased rates of
526 molecular evolution of B class genes in other lineages that have lost petals, for example the
527 Piperaceae and Saururaceae compared with other Piperales (Jaramillo and Kramer, 2007).
528 This likely reflects a release of evolutionary constraints when B class genes no longer need to
529 promote petal identity.
530
531 One interesting observation regarding the expression of UFO is that in *J. curcas*, UFO is
532 downregulated in both mature staminate flowers and mature pistillate flowers compared to
533 younger stages (Chen et al., 2016), whereas in our *E. peplus* dataset we saw the highest
534 expression of UFO in mature staminate flowers. This either suggests a repurposing of UFO, or
535 that developmentally mature but not reproductively mature (i.e. not elongated) staminate flowers
536 in the *E. peplus* cyathium aren't yet transcriptomically mature compared with pistillate flowers.
537 As UFO functions in the development of individual perianth organs as well as in the broader
538 activation of the B class genes (Takeda et al., 2022), some of the changes in UFO expression
539 and sequence in *Euphorbia* could be related to the suppression of perianth development in
540 addition to potential functions in defining the floral meristem.
541

542 Genes in the AP1 clade can also be involved in floral meristem specification– and are also
543 highly diverged in *Euphorbia*. In arabidopsis, AGL79 interacts with SUPPRESSOR OF
544 OVEREXPRESSION OF CONSTANS1 (SOC1) to regulate the expression of TERMINAL
545 FLOWER 1 (TFL1) which controls inflorescence meristem identity (Yang et al., 2023). This AP1
546 (AGL79) homolog in *Euphorbia* appears to have diverged, and now groups in a separate clade
547 within the AP1 clade "missing" its AP1-CAL homolog in the Euphorbiaceae AGL79 clade in our
548 gene tree because that gene, AP1_2, is so diverged that it appears elsewhere in the tree
549 (Supplementary Figure 2).
550
551 One question we had about the cyathium was which other organs might have homology with the
552 filiform structures. In the filiform structures, we observed significant expression of B-class and
553 E-class genes, as well as one homolog of LFY, potentially consistent with floral identity. The
554 filiform structures had low levels of RNA overall compared with other structures in the cyathium
555 (Supplementary File 1), which could be explained by the gene ontology analysis showing
556 significant GO terms relating to heterochromatin formation. Our data therefore agrees with a
557 potential interpretation of the filiform structures as reduced flowers in an inflorescence. Overall,
558 our GO term analysis showed that gene silencing seems to be involved in the creation of
559 multiple cyathium organs.
560
561 The C class gene AGAMOUS is highly expressed in both pistillate flowers and staminate
562 flowers, as would be expected given its function in pistillate and staminate development. We
563 did not see transcriptomic signs of abortion of other whorls in the pistillate and staminate flowers
564 (e.g. hypothetically, seeing B class expression in the young pistillate flower could have been an
565 example of that), besides the upregulation of the putative homolog of the arabidopsis perianth
566 gene KSK in the pistillate flower. Organ abortion can happen at many different stages,

567 however, and unisexual flowers do not always show evidence of their missing whorls (Mitchell
568 and Diggle, 2005).
569
570 In future studies, it would be fruitful to expand this analysis to closely related species given
571 Prenner and Rudall's interpretation of the Australian genus *Calycopeplus* and the New
572 Caledonia tree *Neoguillauminia cleopatra* as "missing links" towards the *Euphorbia* cyathium;
573 future studies could sequence the floral genes of *Calycopeplus*, *Neoguillauminia*, and
574 *Anthostema* to study the sequence evolution of LFY, UFO, AP1 and B class genes with those
575 taxa included to see how much of the sequence divergence occurred in *Euphorbia* alone and
576 how much is shared with these other taxa.
577
578 In addition to expanding our analyses to more taxa, future studies could experimentally
579 investigate the function of the UFO-LFY complex and its DNA binding targets in *Euphorbia*, e.g.
580 through electrophoretic mobility shift assays (EMSA), microscale thermophoresis (MST), or
581 DAP-seq. Additionally, yeast two-hybrid or similar techniques could be used to check the
582 transcription factor binding partners of *Euphorbia*'s B-class genes. It would also be interesting
583 to use ATAC-seq or another method to determine chromatin accessibility across the genome
584 and speculate on what might be being silenced in the different cyathium structures. *In situ*
585 hybridization, if optimized in this system, could also potentially reveal more spatially and
586 temporally resolved patterns of gene expression, including more detailed expression patterns of
587 LFY and UFO. We are excited to see what future work reveals about the developmental
588 genetics involved in creating the complex structure of the cyathium.
589
590
591 **ACKNOWLEDGEMENTS**
592

Thank you to Jacob Landis for extremely helpful advice on running PAML. Thank you to François Parcy, Jérémy Lucas and Laura Turchi for graciously sending the motif files for mLUBS and dLUBS. Thank you to the Cornell Weill growth chamber plant maintenance staff, especially Corbin Lay, for their excellent upkeep of the plants used. Thank you to the Frank Lab for very helpful comments on the manuscript. This work was funded by a Cornell Institute of Biotechnology Seed Grant, National Science Foundation Integrative Organismal Systems (NSF IOS) award 1942437, and startup funds from the College of Agriculture and Life Sciences at Cornell University to Margaret Frank.

AUTHOR CONTRIBUTIONS

A.R.J., A.B., and M.H.F. all conceived of the study. Under the supervision of A.R.J., A.B. collected the images of cyathia and dissected cyathia components, and performed preliminary dissections and RNA extractions that contributed to the experimental design for the RNAseq experiment. A.R.J. performed the dissection for the RNAseq experiment. A.B. and A.R.J. both contributed to the RNA extraction for the RNAseq experiment. A.B. and A.R.J. collaborated on the initial sequence alignment and phylogeny construction to assess conservation of sequence similarity in floral genes. A.R.J. performed all other data analysis. A.R.J. wrote the first draft of the manuscript, after which all authors contributed to reviewing and editing the manuscript.

DATA AVAILABILITY

The raw RNAseq data generated in this study are available from NCBI GenBank under the accession PRJNA1063728. All code used in the data analysis is available on Github at https://github.com/ariellerjohnson/Cyathium-2024.

CONFLICTS OF INTEREST

The authors declare no conflicts of interest.

LITERATURE CITED

Alexa, A., and J. Rahnenfuhrer. 2021. topGO: enrichment analysis for gene ontology. *R package version* 2.46: 2021.

Alvarez, J., and D. R. Smyth. 1999. CRABS CLAW and SPATULA, two Arabidopsis genes that control carpel development in parallel with AGAMOUS. *Development* 126: 2377–2386.

Bailey, T. L., J. Johnson, C. E. Grant, and W. S. Noble. 2015. The MEME Suite. *Nucleic acids research* 43: W39–49.

Bartlett, M. E. 2017. Changing MADS-Box Transcription Factor Protein-Protein Interactions as a Mechanism for Generating Floral Morphological Diversity. *Integrative and comparative biology* 57: 1312–1321.

Bowman, J. L., J. Alvarez, D. Weigel, E. M. Meyerowitz, and D. R. Smyth. 1993. Control of flower development in Arabidopsis thaliana by APETALA1 and interacting genes. *Development* 119: 721–743.

640 Bray, N. L., H. Pimentel, P. Melsted, and L. Pachter. 2016. Near-optimal probabilistic RNA-seq
641 quantification. *Nature biotechnology* 34: 525–527.

642 Brewer, P. B., P. A. Howles, K. Dorian, M. E. Griffith, T. Ishida, R. N. Kaplan-Levy, A. Kilinc, and
643 D. R. Smyth. 2004. PETAL LOSS, a trihelix transcription factor gene, regulates perianth
644 architecture in the Arabidopsis flower. *Development* 131: 4035–4045.

645 Bruyns, P. V. 2022. Euphorbia in Southern Africa: Volume 1. Springer Nature.

646 Buchfink, B., K. Reuter, and H.-G. Drost. 2021. Sensitive protein alignments at tree-of-life scale
647 using DIAMOND. *Nature methods* 18: 366–368.

648 Camacho, C., G. Coulouris, V. Avagyan, N. Ma, J. Papadopoulos, K. Bealer, and T. L. Madden.
649 2009. BLAST+: architecture and applications. *BMC Bioinformatics* 10: 421.

650 Cheng, C.-Y., V. Krishnakumar, A. P. Chan, F. Thibaud-Nissen, S. Schobel, and C. D. Town.
651 2017. Araport11: a complete reannotation of the Arabidopsis thaliana reference genome.
652 *The Plant journal: for cell and molecular biology* 89: 789–804.

653 Chen, M.-S., B.-Z. Pan, Q. Fu, Y.-B. Tao, J. Martínez-Herrera, L. Niu, J. Ni, et al. 2016.
654 Comparative Transcriptome Analysis between Gynoecious and Monoecious Plants
655 Identifies Regulatory Networks Controlling Sex Determination in Jatropha curcas. *Frontiers*
656 *in plant science* 7: 1953.

657 Chen, M.-S., M.-L. Zhao, G.-J. Wang, H.-Y. He, X. Bai, B.-Z. Pan, Q.-T. Fu, et al. 2019.
658 Transcriptome analysis of two inflorescence branching mutants reveals cytokinin is an
659 important regulator in controlling inflorescence architecture in the woody plant Jatropha
660 curcas. *BMC plant biology* 19: 468.

661 Chen, S., Y. Zhou, Y. Chen, and J. Gu. 2018. fastp: an ultra-fast all-in-one FASTQ

662 preprocessor. *Bioinformatics* 34: i884–i890.

663 Claßen-Bockhoff, R., and H. Frankenhäuser. 2020. The 'Male Flower' of Ricinus communis
664 (Euphorbiaceae) Interpreted as a Multi-Flowered Unit. *Frontiers in cell and developmental*
665 *biology* 8: 313.

666 Claßen-Bockhoff, R., and K. Bull-Hereñu. 2013. Towards an ontogenetic understanding of
667 inflorescence diversity. *Ann. Bot.* 112: 1523-1542.

668 Czechowski, T., E. Forestier, S. H. Swamidatta, A. D. Gilday, A. Cording, T. R. Larson, D.
669 Harvey, et al. 2022. Gene discovery and virus-induced gene silencing reveal branched
670 pathways to major classes of bioactive diterpenoids in Euphorbia peplus. *Proceedings of*
671 *the National Academy of Sciences of the United States of America* 119: e2203890119.

672 Dreni, L., and C. Ferrándiz. 2022. Tracing the Evolution of the SEPALLATA Subfamily across
673 Angiosperms Associated with Neo- and Sub-Functionalization for Reproductive and
674 Agronomically Relevant Traits. *Plants* 11.

675 Dreni, L., and M. M. Kater. 2014. MADS reloaded: evolution of the AGAMOUS subfamily genes.
676 *The New phytologist* 201: 717–732.

677 Dreni, L., and D. Zhang. 2016. Flower development: the evolutionary history and functions of
678 the AGL6 subfamily MADS-box genes. *Journal of experimental botany* 67: 1625–1638.

679 Dressler, S., M. Schmidt, and G. Zizka. 2014. Introducing African plants—A photo guide—an
680 interactive photo data-base and rapid identification tool for continental Africa. *Taxon* 63:
681 1159–1161.

682 Emms, D. M., and S. Kelly. 2019. OrthoFinder: phylogenetic orthology inference for comparative
683 genomics. *Genome biology* 20: 238.

684 Favaro, R., A. Pinyopich, R. Battaglia, M. Kooiker, L. Borghi, G. Ditta, M. F. Yanofsky, et al.
685 2003. MADS-box protein complexes control carpel and ovule development in Arabidopsis.
686 *The Plant cell* 15: 2603–2611.

687 Feng, G., B. J. Sanderson, K. Keefover-Ring, J. Liu, T. Ma, T. Yin, L. B. Smart, et al. 2020.
688 Pathways to sex determination in plants: how many roads lead to Rome? *Current opinion in*
689 *plant biology* 54: 61–68.

690 Gagliardi, K. B., I. Cordeiro, and D. Demarco. 2018. Structure and development of flowers and
691 inflorescences in Peraceae and Euphorbiaceae and the evolution of pseudanthia in
692 Malpighiales. *PloS one* 13: e0203954.

693 Gilbert, M. G. 1994. The relationships of the Euphorbieae (Euphorbiaceae). *Annals of the*
694 *Missouri Botanical Garden. Missouri Botanical Garden* 81: 283.

695 Goto, K., and E. M. Meyerowitz. 1994. Function and regulation of the Arabidopsis floral
696 homeotic gene PISTILLATA. *Genes & development* 8: 1548–1560.

697 Grant, C. E., T. L. Bailey, and W. S. Noble. 2011. FIMO: scanning for occurrences of a given
698 motif. *Bioinformatics* 27: 1017–1018.

699 Han, Y., C. Zhang, H. Yang, and Y. Jiao. 2014. Cytokinin pathway mediates *APETALA1*
700 function in the establishment of determinate floral meristems in *Arabidopsis*. *PNAS* 111:
701 6840-6845.

702 Hui, W., Y. Yang, G. Wu, C. Peng, X. Chen, and M. Z. Zayed. 2017. Transcriptome profile
703 analysis reveals the regulation mechanism of floral sex differentiation in Jatropha curcas L.
704 *Scientific reports* 7: 16421.

705 Irish, V. 2017. The ABC model of floral development. *Current biology: CB* 27: R887–R890.

706 Jack, T., L. L. Brockman, and E. M. Meyerowitz. 1992. The homeotic gene APETALA3 of
707 Arabidopsis thaliana encodes a MADS box and is expressed in petals and stamens. *Cell*
708 68: 683–697.

709 Jaramillo, M.A., and E. M. Kramer. 2007. Molecular evolution of the petal and stamen identity
710 genes, *APETALA3* and *PISTILLATA*, after petal loss in the Piperales. *Molecular*
711 *phylogenetics and evolution* 44: 598-609.

712 Jin, R., S. Klasfeld, Y. Zhu, M. Fernandez Garcia, J. Xiao, S.-K. Han, A. Konkol, and D. Wagner.
713 2021. LEAFY is a pioneer transcription factor and licenses cell reprogramming to floral fate.
714 *Nature communications* 12: 626.

715 Jofuku, K. D., B. G. den Boer, M. Van Montagu, and J. K. Okamuro. 1994. Control of
716 Arabidopsis flower and seed development by the homeotic gene APETALA2. *The Plant cell*
717 6: 1211–1225.

718 Johnson, A. R., Y. Yue, S. B. Carey, S. J. Park, L. H. Kruse, A. Bao, A. Pasha, et al. 2023.
719 Chromosome-level genome assembly of Euphorbia peplus, a model system for plant latex,
720 reveals that relative lack of Ty3 transposons contributed to its small genome size. *Genome*
721 *biology and evolution* 15: evad018.

722 Kaplan, D., and C. D. Specht. 2022. Kaplan's Principles of Plant Morphology. CRC Press.

723 Klepikova, A. V., M. D. Logacheva, S. E. Dmitriev, and A. A. Penin. 2015. RNA-seq analysis of
724 an apical meristem time series reveals a critical point in Arabidopsis thaliana flower
725 initiation. *BMC genomics* 16: 466.

726 Kobayashi, Y., H. Kaya, K. Goto, M. Iwabuchi, and T. Araki. 1999. A pair of related genes with
727 antagonistic roles in mediating flowering signals. *Science* 286: 1960–1962.

728 Kolde. Pheatmap: pretty heatmaps. *R package version*.

729 Kozlov, A. M., D. Darriba, T. Flouri, B. Morel, and A. Stamatakis. 2019. RAxML-NG: a fast,
730 scalable and user-friendly tool for maximum likelihood phylogenetic inference.
731 *Bioinformatics* 35: 4453–4455.

732 Lai, X., H. Daher, A. Galien, V. Hugouvieux, and C. Zubieta. 2019. Structural Basis for Plant
733 MADS Transcription Factor Oligomerization. *Computational and structural biotechnology*
734 *journal* 17: 946–953.

735 Lee, H., S. S. Suh, E. Park, E. Cho, J. H. Ahn, S. G. Kim, J. S. Lee, et al. 2000. The
736 AGAMOUS-LIKE 20 MADS domain protein integrates floral inductive pathways in
737 Arabidopsis. *Genes & development* 14: 2366–2376.

738 Levin, J. Z., and E. M. Meyerowitz. 1995. UFO: an Arabidopsis gene involved in both floral
739 meristem and floral organ development. *The Plant cell* 7: 529–548.

740 Li, C., J. Su, X. Liu, S. Chen, and L. He. 2014. Pistillate Flower Development and Stigma
741 Receptivity of Euphorbia pulcherrima. *Agricultural Science & Technology* 15: 1671–1675.

742 Liljegren, S. J., G. S. Ditta, Y. Eshed, B. Savidge, J. L. Bowman, and M. F. Yanofsky. 2000.
743 SHATTERPROOF MADS-box genes control seed dispersal in Arabidopsis. *Nature* 404:
744 766–770.

745 Lippman, Z. B., O. Cohen, J. P. Alvarez, M. Abu-Abied, I. Pekker, I. Paran, Y. Eshed, and D.
746 Zamir. 2008. The making of a compound inflorescence in tomato and related nightshades.
747 *PLoS biology* 6: e288.

748 Litt, A., and E. M. Kramer. 2010. The ABC model and the diversification of floral organ identity.
749 *Seminars in cell & developmental biology* 21: 129–137.

750 Liu, J., C. Shi, C.-C. Shi, W. Li, Q.-J. Zhang, Y. Zhang, K. Li, et al. 2020. The Chromosome-
751 Based Rubber Tree Genome Provides New Insights into Spurge Genome Evolution and
752 Rubber Biosynthesis. *Molecular plant* 13: 336–350.

753 Love, M. I., W. Huber, and S. Anders. 2014. Moderated estimation of fold change and
754 dispersion for RNA-seq data with DESeq2. *Genome biology* 15: 550.

755 Machanick, P., and T. L. Bailey. 2011. MEME-ChIP: motif analysis of large DNA datasets.
756 *Bioinformatics* 27: 1696–1697.

757 Ma, H., M. F. Yanofsky, and E. M. Meyerowitz. 1991. AGL1-AGL6, an Arabidopsis gene family
758 with similarity to floral homeotic and transcription factor genes. *Genes & development* 5:
759 484–495.

760 Mandel, M. A., and M. F. Yanofsky. 1995. The Arabidopsis AGL8 MADS box gene is expressed
761 in inflorescence meristems and is negatively regulated by APETALA1. *The Plant cell* 7:
762 1763–1771.

763 Miller, C. N., J. Dumenil, F. H. Lu, C. Smith, N. McKenzie, V. Chapman, J. Ball, et al. 2020.
764 Variation in the expression of a transmembrane protein influences cell growth in
765 Arabidopsis thaliana petals by altering auxin responses. *BMC plant biology* 20: 482.

766 Mitchell, C. H., and P. K. Diggle. 2005. The evolution of unisexual flowers: morphological and
767 functional convergence results from diverse developmental transitions. *American journal of*
768 *botany* 92: 1068–1076.

769 Mizukami, Y., and H. Ma. 1997. Determination of Arabidopsis floral meristem identity by
770 AGAMOUS. *The Plant cell* 9: 393–408.

771 Morel, P., P. Chambrier, V. Boltz, S. Chamot, F. Rozier, S. Rodrigues Bento, C. Trehin, et al.

2019. Divergent Functional Diversification Patterns in the SEP/AGL6/AP1 MADS-Box Transcription Factor Superclade. *The Plant cell* 31: 3033–3056.

Morel, P., K. Heijmans, K. Ament, M. Chopy, C. Trehin, P. Chambrier, S. Rodrigues Bento, et al. 2018. The Floral C-Lineage Genes Trigger Nectary Development in Petunia and Arabidopsis. *Plant Cell* 30: 2020–2037.

Moyroud, E., E. Kusters, M. Monniaux, R. Koes, and F. Parcy. 2010. LEAFY blossoms. *Trends in plant science* 15: 346–352.

O'Brien, M., R. N. Kaplan-Levy, T. Quon, P. G. Sappl, and D. R. Smyth. 2015. PETAL LOSS, a trihelix transcription factor that represses growth in Arabidopsis thaliana, binds the energy-sensing SnRK1 kinase AKIN10. *Journal of experimental botany* 66: 2475–2485.

Pelaz, S., G. S. Ditta, E. Baumann, E. Wisman, and M. F. Yanofsky. 2000. B and C floral organ identity functions require SEPALLATA MADS-box genes. *Nature* 405: 200–203.

Prenner, G., N. I. Cacho, D. Baum, and P. J. Rudall. 2010. Is LEAFY a useful marker gene for the flower–inflorescence boundary in the Euphorbia cyathium? *Journal of experimental botany* 62: 345–350.

Prenner, G., S. D. Hopper, and P. J. Rudall. 2008. Pseudanthium development in Calycopeplus paucifolius, with particular reference to the evolution of the cyathium in Euphorbieae (Euphorbiaceae–Malpighiales). *Australian systematic botany* 21: 153–161.

Prenner, G., and P. J. Rudall. 2007. Comparative ontogeny of the cyathium in Euphorbia (Euphorbiaceae) and its allies: exploring the organ-flower-inflorescence boundary. *American journal of botany* 94: 1612–1629.

Quinlan, A. R., and I. M. Hall. 2010. BEDTools: a flexible suite of utilities for comparing genomic

794 features. *Bioinformatics* 26: 841–842.

795 Rieu, P., M. Arnoux-Courseaux, G. Tichtinsky, and F. Parcy. 2023a. Thinking outside the F-box:
796 how UFO controls angiosperm development. *The New phytologist* 240: 945–959.

797 Rieu, P., L. Turchi, E. Thévenon, E. Zarkadas, M. Nanao, H. Chahtane, G. Tichtinsky, et al.
798 2023b. The F-box protein UFO controls flower development by redirecting the master
799 transcription factor LEAFY to new cis-elements. *Nature plants* 9: 315–329.

800 Robert, X., and P. Gouet. 2014. Deciphering key features in protein structures with the new
801 ENDscript server. *Nucleic acids research* 42: W320–4.

802 Rodríguez-Pelayo, C., B. A. Ambrose, A. Vasco, J. F. Alzate, and N. Pabón-Mora. 2022.
803 Evolution and expression of LEAFY genes in ferns and lycophytes. *EvoDevo* 13: 2.

804 Schmitz, R. J., L. Hong, S. Michaels, and R. M. Amasino. 2005. FRIGIDA-ESSENTIAL 1
805 interacts genetically with FRIGIDA and FRIGIDA-LIKE 1 to promote the winter-annual habit
806 of Arabidopsis thaliana. *Development* 132: 5471–5478.

807 Schultz, E. A., and G. W. Haughn. 1991. LEAFY, a Homeotic Gene That Regulates
808 Inflorescence Development in Arabidopsis. *The Plant cell* 3: 771–781.

809 Shen, W., S. Le, Y. Li, and F. Hu. 2016. SeqKit: A Cross-Platform and Ultrafast Toolkit for
810 FASTA/Q File Manipulation. *PloS one* 11: e0163962.

811 Slavković, F., C. Dogimont, H. Morin, A. Boualem, and A. Bendahmane. 2021. The Genetic
812 Control of Nectary Development. *Trends in plant science* 26: 260–271.

813 Souer, E., A. B. Rebocho, M. Bliek, E. Kusters, R. A. M. de Bruin, and Ronald Koes. 2008.
814 Patterning of Inflorescences and Flowers by the F-Box Protein DOUBLE TOP and the
815 LEAFY Homolog ABERRANT LEAF AND FLOWER of Petunia. *The Plant Cell* 20: 2033-

816 2048.

817 Supek, F., M. Bošnjak, N. Škunca, and T. Šmuc. 2011. REVIGO summarizes and visualizes
818 long lists of gene ontology terms. *PloS one* 6: e21800.

819 Takeda, S., Y. Hamamura, T. Sakamoto, S. Kimura, M. Aida, and T. Higashiyama. 2022. Non-
820 cell-autonomous regulation of petal initiation in Arabidopsis thaliana. *Development* 149.

821 Tang, M., Y.-B. Tao, Q. Fu, Y. Song, L. Niu, and Z.-F. Xu. 2016. An ortholog of LEAFY in
822 Jatropha curcas regulates flowering time and floral organ development. *Scientific reports* 6:
823 37306.

824 Tuskan, G. A., S. Difazio, S. Jansson, J. Bohlmann, I. Grigoriev, U. Hellsten, N. Putnam, et al.
825 2006. The genome of black cottonwood, Populus trichocarpa (Torr. & Gray). *Science* 313:
826 1596–1604.

827 Valliyodan, B., S. B. Cannon, P. E. Bayer, S. Shu, A. V. Brown, L. Ren, J. Jenkins, et al. 2019.
828 Construction and comparison of three reference-quality genome assemblies for soybean.
829 *The Plant journal: for cell and molecular biology* 100: 1066–1082.

830 Wang, M., Z. Gu, Z. Fu, and D. Jiang. 2021. High-quality genome assembly of an important
831 biodiesel plant, Euphorbia lathyris L. *DNA research: an international journal for rapid*
832 *publication of reports on genes and genomes* 28.

833 Weigel, D., J. Alvarez, D. R. Smyth, M. F. Yanofsky, and E. M. Meyerowitz. 1992. LEAFY
834 controls floral meristem identity in Arabidopsis. *Cell* 69: 843–859.

835 Western Australian Herbarium, Biodiversity, Conservation Science, Department of Biodiversity,
836 Conservation, and Attractions. Calycopeplus Planch. Website
837 https://florabase.dbca.wa.gov.au/browse/profile/21684 [accessed 25 January 2024].

838 Xanthopoulou, A., J. Montero-Pau, B. Picó, P. Boumpas, E. Tsaliki, H. S. Paris, A. Tsaftaris, et
839 al. 2021. A comprehensive RNA-Seq-based gene expression atlas of the summer squash
840 (Cucurbita pepo) provides insights into fruit morphology and ripening mechanisms. *BMC*
841 *genomics* 22: 341.

842 Xu, G., J. Huang, Y. Yang, and Y.-A. Yao. 2016. Transcriptome Analysis of Flower Sex
843 Differentiation in Jatropha curcas L. Using RNA Sequencing. *PloS one* 11: e0145613.

844 Xu, W., D. Wu, T. Yang, C. Sun, Z. Wang, B. Han, S. Wu, et al. 2021. Genomic insights into the
845 origin, domestication and genetic basis of agronomic traits of castor bean. *Genome biology*
846 22: 113.

847 Yang, H., P. Zhang, D. Guo, N. Wang, H. Lin, X. Wang, and L. Niu. 2023. Transcriptional
848 repressor AGL79 positively regulates flowering time in Arabidopsis. *Journal of plant*
849 *physiology* 285: 153985.

850 Zhang, T. and P. Elomaa. 2021. Don't be fooled: false flowers in Asteraceae. *Current opinion*
851 *in plant biology* 59: 101972.

852 Zhang, T., Y. Zhao, I. Juntheikki, K. Mouhu, S. K. Broholm, A. S. Rijpkema, L. Kins, T. Lan, V.
853 A. Albert, T. H. Teeria, and P. Elomaa. 2017. Dissecting functions of *SEPALLATA*-like
854 MADS box genes in patterning of the pseudanthial inflorescence of *Gerbera hybrida*. *New*
855 *phytologist* 216: 939-954.

856 Zhang, X., L. Pan, W. Guo, Y. Li, and W. Wang. 2022. A convergent mechanism of sex
857 determination in dioecious plants: Distinct sex-determining genes display converged
858 regulation on floral B-class genes. *Frontiers in plant science* 13: 953445.

859 Zhao, Y., T. Zhang, S. K. Broholm, S. Tähtiharju, K. Mouhu, V. A. Albert, T. H. Teeri, and P.
860 Elomaa. 2016. Evolutionary Co-Option of Floral Meristem Identity Genes for Patterning of

861 the Flower-Like Asteraceae Inflorescence. *Plant physiology* 172: 284-296.

862 Zumajo-Cardona, C., and N. Pabón-Mora. 2016. Evolution of the APETALA2 Gene Lineage in
863 Seed Plants. *Molecular biology and evolution* 33: 1818–1832.

864

865

866 **FIGURE LEGENDS**

867

868 Figure 1: The *Euphorbia* cyathium is a unique reproductive structure. A. Diagram of a *Euphorbia*
869 *peplus* cyathium; involucre is cut away to reveal filiform structures and staminate flowers inside.
870 B. *E. peplus* cyathium and adjacent primordia and cyathophylls. Scale=2mm. C. *E. peplus*
871 cyathium and adjacent primordia with adjacent cyathophylls removed. Scale=1mm. D. *E.*
872 *peplus* cyathium with involucre and nectaries removed. Scale=500 microns. E. Diagram of the
873 ABCDE model of floral development and the four whorls of a traditional flower; D class genes,
874 which control ovule development, are not shown.

875

876 Figure 2: Close relatives of *Euphorbia*, *Calycopeplus* and *Neoguillauminia*, have perianths
877 around their pistillate and staminate flowers and a condensed inflorescence similar to that of
878 *Euphorbia*. *Anthostema*, which is less closely related, has perianths around its pistillate and
879 staminate flowers and a less-condensed inflorescence.

880

881 Figure 3: Staminate flowers have a distinct expression pattern. A-D. Illustration of cyathium
882 parts used for RNAseq sampling. A. Small primordium. B. Large primordium. C. Young
883 staminate flower and young pistillate flower. D. Mature organs: nectary, involucre, staminate
884 flower, pistillate flower, filiform structure, involucre, nectary. (Duplicates of organs are omitted
885 for simplicity. Cyathophyll is not shown.) E. PCA plot of variance-stabilized-transformed data

886 for the 500 genes with the most variance. PC1 explains 22.4% of the variance, PC2 explains
887 18.9% of the variance, PC3 explains 16.7% of the variance, and PC4 explains 10.6% of the
888 variance.
889
890 Figure 4: E class gene SEP3 is highly expressed in the pistillate and staminate flowers. A.
891 Heatmap shows expression of ABCDE homologs and other floral identity genes in different
892 organs of the *E. peplus* cyathium. B-N. Images of the organs sampled. B. Young pistillate
893 flower. C. Young staminate flower. D. Nectary. E. Filiform structure. F. Mature pistillate flower.
894 G. Mature staminate flower. Scale bars = 250 microns.
895
896 Figure 5: Biological Process GO terms for genes significantly upregulated in the nectary,
897 involucre, and filiform structures as compared with the cyathophyll and Molecular Function GO
898 terms for genes significantly upregulated in the nectary as compared with the cyathophyll are
899 summarized using REVIGO. "Value" is the log10(p-value); a lower value, towards the red side
900 of the color scale, is more significant. The size of the points, the dispensability, represents the
901 semantic similarity to other terms in the dataset.
902
903 Figure 6: LFY, UFO, and B class genes show signs of divergence and relaxed selection in
904 *Euphorbia*. A. dN/dS values shown on gene trees of floral genes of interest; RAxML support
905 value from 1000 bootstraps is shown at nodes. PHYA is shown as a non-floral "control". B.
906 Visualization of amino acid alignment in a highly conserved region of LFY; site 279 is a DNA
907 binding site that is highly conserved (except in *Euphorbia*). Cyan color shows sites in the LFY
908 protein alignment rated as "highly significant" for positive selection in the *Euphorbia* clade by
909 PAML. C. Visualization of amino acid alignment at the start of the UFO protein showing
910 deletions in *Euphorbia* ("Ep" and "Casp" genes). Gene names and their gene ID equivalents are
911 listed in Supplementary File 3.

912 **SUPPLEMENTAL DATA FILE TITLES**

913

914 Supplementary Figures (combined into a single PDF)

915 Supplementary File 1—Sequence statistics

916 Supplementary File 2—Orthogroups

917 Supplementary File 3—Gene names

918 Supplementary File 4—DESeq data

919 Supplementary File 5—Differential expression

920 Supplementary File 6—E. peplus GO terms

921 Supplementary File 7—TopGO results

922 Supplementary File 8—Positive selection sites

923 Supplementary File 9—Motif search results